



RESEARCH ON THE CONSTRUCTION AND APPLICATION OF ELECTRICAL FAULT CLASSIFICATION SYSTEM BASED ON BAYESIAN ALGORITHM

Xiaowei ZHANG ¹ , Mingdong ZHU ² 

¹ Xuchang Vocational and Technical College, College of Mechatronics and Engineering. No. 4336, Xinxing East Road, Dongcheng District, Xuchang City, Henan Province, China

² Xuchang Vocational Technical College, College of Mechatronics and Automotive Engineering. No. 4336, Xinxing East Road, Dongcheng District, Xuchang City, Henan Province, China

*Corresponding author, e-mail: 13193461627@163.com

Abstract

With the rapid development of smart building technology, the safe and stable operation of the electrical system has become the core demand of modern building management. This study aims to construct an automated classification system for electrical faults based on Bayesian algorithm to improve the accuracy and efficiency of fault diagnosis. First, the wavelet transform is utilized for noise reduction and feature extraction of electrical signals to enhance the signal-to-noise ratio of the data. Subsequently, multi-category fault diagnosis is realized based on association vector machine, and Bayesian approach is combined to quantify the uncertainty factors and improve the classification reliability. The results show that the system performs well with small sample data, and the average recognition accuracy of various types of faults exceeds 70%. The wavelet transform-based fault recognition method demonstrates high stability, with the highest accuracy reaching 100% and the lowest still maintaining around 90%. In addition, the Bayesian classifier significantly improves the confidence level of fault diagnosis after parameter optimization, which verifies the effectiveness of the algorithm. It provides a feasible solution for the fault prediction and health management of power systems in intelligent buildings.

Keywords: support vector machine; artificial intelligence; electrical fault; diagnosis

1. INTRODUCTION

The White Paper on Intelligent Design of Buildings by 2020 indicates that Chinese smart architecture is developing continuously [1]. Due to the increasingly complicated electric system, the conventional detecting technique can't satisfy the request of [2], so it becomes more and more important to improve it.

Error is defined as the magnitude of the difference found, or the deviation of the calculation parameters from an acceptable margin [3]. The reliability and effectiveness of diagnostic results as well as are demonstrated in the course of failure diagnosis of construction electric system [4]. The construction electric system is one of the management system for the construction power consumption.

In the construction electrical system, if any fault occurs, the machine will be stopped and the data will be lost. With the development of technological progress, the construction electrical system is more complex, resulting in a variety of more complex faults. Therefore, in order to ensure the safety of

construction electrical equipment, we should pay attention to the study of fault diagnosis of construction electrical system.

The electrical faults of the building mainly include line faults, electrical components and device faults, lightning and grounding faults. The essence of the fault detection of building power system is to extract and determine [5-6]. The causes of building electrical equipment failure mainly include design defects, improper installation, equipment aging, environmental factors, operation errors, power supply problems and external factors. Unreasonable design or unqualified specifications may lead to overload operation of equipment; the installation error or poor grounding may affect the normal operation of equipment; long-term use reduces insulation performance and wear of components; bad environment such as humidity and high temperature accelerate equipment aging; misoperation or improper maintenance increase fault risk; power supply problems such as voltage fluctuation and harmonic interference damage equipment; external events such as lightning strike and short circuit may

also cause failure. Regular maintenance and standard operation are the key to reducing faults [7].

For building electrical system diagnosis and classification of fault must have correct fault data, and accurate analysis, need to collect more data from building electrical system, mainly for current, voltage, harmonic fault signal acquisition, which can provide real-time and accurate fault data for building electrical system, so the data collection is also very important [8].

The diagnostic methods of building electrical equipment include visual inspection, instrument detection, infrared thermal imaging, ultrasonic detection, on-line monitoring and fault recording analysis. Visual inspection is simple and intuitive but limited to surface problems; instrument detection is accurate but requires expertise; infrared thermal imaging can find overheating problems but equipment is expensive; ultrasonic detection is suitable for local discharge but susceptible to noise interference; online monitoring real-time warning but high cost; fault recording analysis is suitable for complex faults but requires professional analysis [9]. The integrated use of multiple methods can improve the diagnostic efficiency. However, the current diagnostic methods of building electrical equipment have the problems of insufficient data quality and diversity, small samples, insufficient algorithm complexity and real-time performance, insufficient multi-modal data fusion, poor model interpretability, and environmental interference and noise. Poor data quality and insufficient samples affect the training effect of the model, complex algorithms are difficult to meet the real-time requirements, a single data source limits the comprehensiveness of diagnosis, the lack of interpretation of the black-box model reduces the credibility, and environmental noise interference leads to data distortion [10]. The improvement direction includes data cleaning and enhancement, multi-modal data fusion, lightweight algorithm optimization, the introduction of explanatory artificial intelligence technology and the application of signal processing technology to improve the diagnostic accuracy, real-time and practicability [11-12].

Therefore, in order to study the electrical fault classification system, this paper proposes the automatic classification system of electrical fault and Bayesian algorithm based on SVM and compression sensing algorithm, and tests the application results, to prove that it has good diagnosis and identification ability. The automatic electrical fault classification system will provide important support for the safe operation and efficient management of the power system, which has wide application prospects and social value.

2. ELECTRICAL FAULT DIAGNOSIS ALGORITHM

2.1. Electrical fault diagnosis algorithm based on wavelet transform and support vector machine (WT-SVM)

(1) Wavelet transform

Firstly, the fuzzy image is divided into low-frequency and high-frequency sub-bands by means of multi-resolution analyzing capability. The low-frequency portion includes a large portion of the fog image, while the high-frequency portion is associated with the detail portion of the picture.

Two-dimensional images can be decomposed into four sub-images by wavelet decomposition:

$$L_i f(x, y) = f(x, y), \phi_{j,m}(x) > \phi_{j,m}(y) \quad (1)$$

$$H_j^1 f(x, y) = f(x, y), \phi_{j,n}(x) > \psi_{j,m}(y) \quad (2)$$

$$H_j^2 f(x, y) = f(x, y), \psi_{j,n}(x) > \phi_{j,m}(y) \quad (3)$$

$$H_j^3 f(x, y) = f(x, y), \psi_{j,n}(x) > \psi_{j,m}(y) \quad (4)$$

Where ϕ , wavelet function and scale function respectively; $L_i f(x, y)$ is the approximation of the original image, namely low frequency information; $H_j^1 f(x, y)$ ($t = 1, 2, 3$) is the high frequency part of the image; $H_j^1 f(x, y)$ is the horizontal edge information; $H_j^2 f(x, y)$ is the vertical edge information; $H_j^3 f(x, y)$ is the high frequency information in the diagonal direction.

Figure 1 is a schematic diagram of the wavelet decomposition, with the wavelet reconstruction performed according to the opposite process. LL 1 represents the low-frequency subband map of the original image, which maintains the main information of the original image and concentrates the noise of the original image; HL1 is the subband map of the horizontal edge information; LH-1 is a high frequency sub-band image of the vertical edge, and HH1 is a high frequency sub-band image of the integrated information in the diagonal. The HF sub-band can be used to represent the details of the picture. Therefore, it is very important to improve the HF sub-band. Another decomposition of LL 1 yields four subimages of LL 2, HL2, LH 2, and HH 2.

(2) Support Vector Machine SVM

The basic model of machine learning, can be shown in the figure 1.

The generator is the source, producing the random vector $x \in R^n$, which is generated from an independent and identical distribution of an unknown but fixed probability distribution function $F(x)$.

The vector x produced by the generator, input into the trainer, gives the output value y . The input and output vectors form the training samples (x, y) during the training process.

After learning the training set of machine observations, for the internal relationship between the training samples, a certain operator is constructed, predicting the predicted samples, and the output y' .

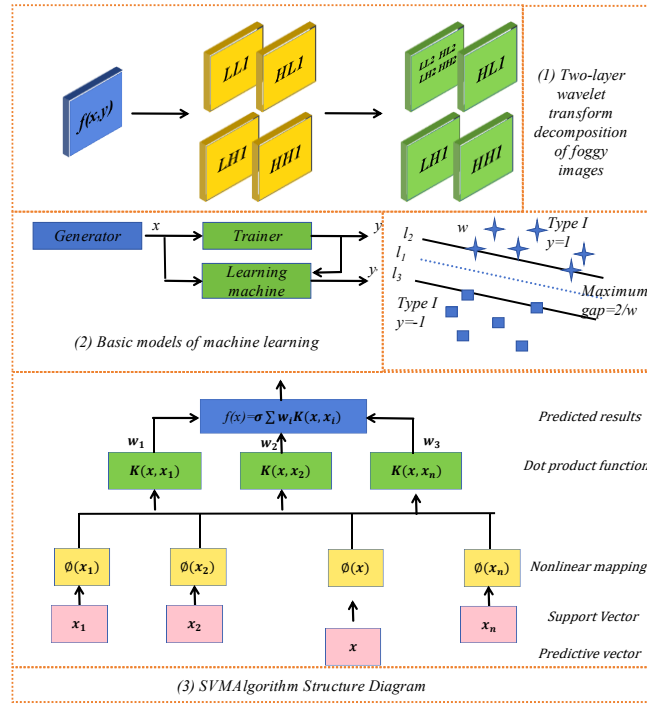


Fig. 1. Structural diagram of wavelet transform and support vector machine

The essence of the fault diagnosis problem is actually a pattern recognition problem [13]. To judge that the operation state of the equipment is normal or abnormal, the fault form of the equipment or the specific location of the fault itself are all pattern recognition problems, or classification problems. The initial study of SVM was proposed for two classes of linear separable problems in pattern recognition, with the aim of finding a hyperplane that completely separates the two classes of samples.

And practical application, to two kinds of samples correct classification of superplane, and we want to get is not only the two types of samples correctly, and make each kind of data and the hyperplane distance of the nearest point and the distance of the superplane, also become the largest classification spacing, the superplane is called the optimal hyperplane [14].

A line l with w as the normal vector can correctly classify two types of points, but such lines are not unique, but can also be moved in parallel until the input of a training point, thus obtaining two extreme lines l_2 and l_3 , called these two lines as supporting lines. All parallel lines in the support line can correctly classify the two categories, while the line l_1 between the support lines l_2 and l_3 is best. In choosing the law of splitting a linear line, it is necessary to consider that if there is an appropriate law, there will be two supporting lines, which are known as the "gap". In fact, we must choose the law direction which can maximize the "space". It is also known as the maximal interval principle.

The candidate line l is set as first

$$(w \cdot x) + b = y \tag{5}$$

Then the two supporting straight lines can be expressed as

$$(w \cdot x) + b = 1 \tag{6}$$

$$(w \cdot x) + b = -1 \tag{7}$$

The desired l_1 should be

$$(w \cdot x) + b = 0 \tag{8}$$

At this time, the corresponding two supporting lines are separated by $\frac{2}{\|w\|}$

The idea of the maximum interval principle leads to solving the following optimization problems for w and b .

$$\max_{w,b} \frac{2}{\|w\|} + C \sum_{i=1}^n \xi_i \tag{9}$$

$C \sum_{i=1}^n \xi_i$ is the penalty term, used to control the degree of classification error.

C is a hyperparameter used to balance the weights between interval maximization and classification errors. Larger C indicates a heavier penalty for classification errors; smaller C indicates that more classification errors are allowed.

s. t. For all make $y_i = 1$ Get under the bid i

$$(w \cdot x_i) + b \geq 1 - \xi_i \tag{10}$$

For all make $y_i = -1$ Get under the bid i

$$(w \cdot x_i) + b \leq -1 \tag{11}$$

$$\min_{w,b} \frac{1}{2} \|w\|^2 \tag{12}$$

$$y_i((w \cdot x_i) + b) \geq 1, i = 1, \dots, k \tag{13}$$

In the SVM approach, consider another way to achieve the maximum interval,

Instead of directly solving the above optimization problem, but by solving the solution to its dual problem.

According to the optimal solution, w' , b' , the desired line can be obtained

$$(w' \cdot x) + b' = 0 \tag{14}$$

$$f(x) = \text{sgn}((w' \cdot x) + b') \tag{15}$$

The dual problem of the above problem is introduced here:

$$\max \alpha - \frac{1}{2} \sum_{i=1}^k \sum_{j=1}^k y_i y_j (x_i \cdot x_j) \alpha_i \alpha_j + \sum_{j=1}^k \alpha_j \tag{16}$$

$$\text{s.t. } \sum_{i=1}^l y_i \alpha_i = 0 \quad (17)$$

$$\alpha_i \geq 0, i = 1, \dots, k \quad (18)$$

SVM was initially developed as a method for dealing with two kinds of classification problems, then it was expanded into regression domain. Regarding the non-separable property, Vapnik and his colleagues proposed the kernel space theory, which can be used to map low dimension data into high dimension by non-linear mapping. If we choose proper mapping, we can convert the non-separable input space into linear separability problem. With the deep and extensive research of SVM, many new and improved algorithms are produced in the practical application process, such as C-SVM, B-SVM, V-SVM, LS-SVM and other [15].

① C-SVM algorithm

In the training vector $x_i = 1, L, k$, belong to two kinds of problems, namely, $\{1,1\}$, y_i this initial problem is:

$$\min \frac{1}{2} w^T w + C \sum_{i=1}^k \xi_i \quad (19)$$

$$y_i(w^T \phi(x_i) + b) \geq 1 - \xi_i, \quad \xi_i \geq 0, \quad i = 1, \dots, k \quad (20)$$

In the above equation, C represents the penalty coefficient, the larger it means, the greater the penalty for misclassification, thus improving the classification accuracy. C is the adjustable parameter in the algorithm, which is called C-SVM algorithm. C-SVM algorithm is the most basic SVM algorithm, and many algorithms are different extensions.

② BSVM algorithm

The BSVM (Bounded SVM) is actually a deformation of the C-SVM algorithm, which is mainly added to the original objective function

For the $\frac{b^2}{2}$ term, the initial problem after the deformation is as follows:

$$\min \frac{1}{2} w^T w + C \sum_{i=1}^k \xi_i + \frac{b^2}{2} \quad (21)$$

$$y_i(w^T \phi(x_i) + b) \geq 1 - \xi_i, \quad \xi_i \geq 0, \quad i = 1, \dots, k \quad (22)$$

Compared with the C-SVM algorithm, BSVM has one more optimization goal, but the constraint condition has one less equation constraint, which becomes a quadratic programming problem under the boundary constraint, which is more suitable for iterative solution. It also increases the convergence rate.

③ v-SVM algorithm

The v-SVM algorithm uses the new parameter v to control the number and error of support vectors, thus solving the defect that it is difficult to choose correctly in practical application because the parameter C in the C-SVM algorithm is not intuitively explained. And v has clear physical meaning and is easy to choose, thus improving the performance of SVM. Thus the initial problem can be described as:

$$\min_{w,b,\rho,\xi_i} \frac{1}{2} w^T w - v\rho + C \sum_{i=1}^k \xi_i \quad (23)$$

$$y_i(w^T \phi(x_i) + b) \geq \rho - \xi_i, \quad \xi_i \geq 0, \quad i = 1, \dots, k \quad \rho \geq 0 \quad (24)$$

Of these, there is $0 < v < 1$. The v-SVM for classification is proposed by Scholkopf, which has some advantages over the C-SVM, but there are two equality constraints in its dual problem, so the

solution is more complicated. C. Chang et al. After a deep study of C-SVM and v-SVM pointed out that v is a minus function of C, and thus designed a similar training algorithm.

2.2 Electrical fault diagnosis algorithm based on compression sensing and K-nearest neighbor (CS-KNN)

(1) Compression-sensing fault diagnosis method

SVM was initially developed as a method for dealing with two kinds of classification problems, then it was expanded into regression domain. Regarding the non-separable property, Vapnik and his colleagues proposed the kernel space theory, which can be used to map low dimension data into high dimension by non-linear mapping. If we choose proper mapping, we can convert the non-separable input space into linear separability problem:

$$A_i = [v_{i,1} \quad v_{i,2} \quad \dots \quad v_{i,n_i}] \in \mathbf{R}^{p \times n_i} \quad (25)$$

Where: v_{ij} is the jth training sample of class I failure, and A_i is the training sample matrix of class I failure.

Because the sample is not known, it is possible to combine n training samples from each of the k-classes into a full training matrix A:

$$A = [A_1 \quad \dots \quad A_i \quad \dots \quad A_k] = [v_{1,1} \quad \dots \quad v_{1,n_1} \quad \dots \quad v_{i,n_i} \quad \dots \quad v_{k,n_k}] \quad (26)$$

$$y = v_{i,1} + a_{i,2}v_{i,2} + \dots + a_{i,n_i}v_{i,n_i} \quad (27)$$

Where: $a_{i,j}$ and j is the weight coefficient.

When a fault test data y is given, the category of the sample is unknown, and it is the fault in the sample set. Therefore, the fault to be classified is linearly represented by the complete matrix A y:

$$y = a_{1,1}v_{1,1} + \dots + a_{1,n_1}v_{1,n_1} + \dots + a_{i,1}v_{i,1} + \dots + a_{i,n_i}v_{i,n_i} + \dots + a_{i,1}v_{i,1} + \dots + a_{k,n_k}v_{k,n_k} \quad (28)$$

$$y = AX \quad (29)$$

The matrix can be solved by using Equation (30):

$$X = [a_1 \quad a_2 \quad \dots \quad a_i] \quad (30)$$

If a given y belongs to class i, then y only needs to be expressed by the sample data of class i, then

$$X = [0 \quad \dots \quad 0 \quad a_{i,1} \quad \dots \quad a_{i,n_i} \quad 0 \quad \dots \quad 0]^T \quad (31)$$

Therefore, the coefficient of X is theoretically only a_i not 0, and the other k-1 coefficients are 0, so that X is a sparse vector, which can be regarded as a sparse decomposition of the test sample y.

If a given unknown test sample is required to be classified, then the category of faults to be classified can be known as long as the sparse vector X is solved for each y according to Equation (31), and only the n_i coefficient related to the tested sample on X. In practice, we use the method of solving L1 minimization to get an accurate or approximate approach for X, but it doesn't work well in theory. In order to complete the classification work through the value of X, the following classification function should be used:

$$\min_i r_i(y) = \|y - A\delta_i(x)\|_2 \quad (32)$$

Where $i = 1, 2, \dots, k$, $\delta_i(x)$ is the element of the row associated with class I in the pointing quantity x. If the m value is minimum $[1, k]$, the test sample y is a class m failure.

(2) Algorithm training

In this thesis, we have taken 55 samples from the experiment station, and we have obtained five kinds of status patterns (line impedance failure, continuous failure, unusual earthing resistance, low isolation resistance, and normal). Among them, a single specimen was chosen at random for every kind of failure, while the other 50 were used as training specimens. Fifty groups of tests are repeated, and then the mean value is used to estimate the precision of the last classification. This section of the test is performed on a dual core processor at 2.13 GHz.

Based on the experiment plan and procedure, the matrix size in Formula (4-9) is 10 x 50, and the test specimen is 10x1. Figure 2 illustrates the test results. Fig. 2 (1) shows the sparsity of X, which is computed with L and a classifier (this value takes a test specimen that is part of a line-impedance error (E1)). Fig. 2 (2) shows the last five remaining conditions, which are computed according to Equation (32).

The horizontal axis of Figure 2 is the number of type 5 fault state, 1-10 is class 1 line impedance fault, 11-20 is type 2 continuous fault, 21-30 is type 3 abnormal grounding resistance, 31-40 is class 4 low insulation resistance, 41-50 is type 5 normal state. The vertical axis is the projection-sparse expression coefficient on the training sample for the test sample solved under the L minimization norm. As shown in the figure, when the test data is selected from the first type fault sample, the final sparse representation vector is indeed sparse, and the location of the maximum coefficient is corresponding to the first type fault training data, it is intuitively judged that the test sample should belong to the first type fault.

When the sparse representation coefficient x is obtained, because of the sparsity, the corresponding test sample belonging class can be determined by finding non-zero terms from x. However, in practical problems, it is often difficult to get a non-zero value, so if there are two or more non-zero value in x, can calculate the linear weighted residual value m (y) through each fault sample formula (4-11), the result is shown in Figure 4-5, after comparing the residual value, take the smallest value category 1 as the final diagnosis classification result.

3. ELECTRICAL FAULT CLASSIFICATION ALGORITHM

3.1. Research on building electrical fault classification based on the Bayesian method

(1) Theory of algorithm

The main ideological basis of naive Bayesian classification is: for the given item to be classified, solve the probability of each category under the condition of this item appears, and select the category with the largest probability as the attribution category [16] of the item to be classified. The naive Bayes classifier needs to seek the hypothetical category with the greatest likelihood in the sample data set D, and this hypothesis with the greatest likelihood is called the maximal posterior (Maximum A Posteriori, or MAP) hypothesis [17]. We used the Bayesian formula to calculate the posterior probability of each candidate hypothesis to determine the maximum posterior hypothesis MAP:

$$h_{MAP} = \underset{h \in H}{argmax} p(h | D) \tag{33}$$

Where H is the set of candidate hypotheses, according to the Bayesian formula:

$$h_{MAP} = \underset{h \in H}{argmax} \frac{p(D|h)p(h)}{p(D)} \tag{34}$$

Since p(D) is a constant, formula 3-3 can be simplified:

$$h_{MAP} = \underset{h \in H}{argmax} p(D | h)p(h) \tag{35}$$

Then, for a certain set of data set D, we can convert the classification question into MAP assumption.

A collection of property values is used to represent the data sample X, whereas a category mark c receives a value from a limited set C. Predict its class markers based on the training sample set and test data samples. In a given case, the Bayesian classifier needs to find the assumption that the likelihood is greatest given a set of instances, and the goal of solving the test data sample x under the maximum posterior assumption is to obtain the most likely class marker c(x) given the attribute value of the described instance. Its equations such as:

$$c(x) = \underset{ccc}{argmax} p(a_1, a_2, \dots, a_n | c) p(c) \tag{36}$$

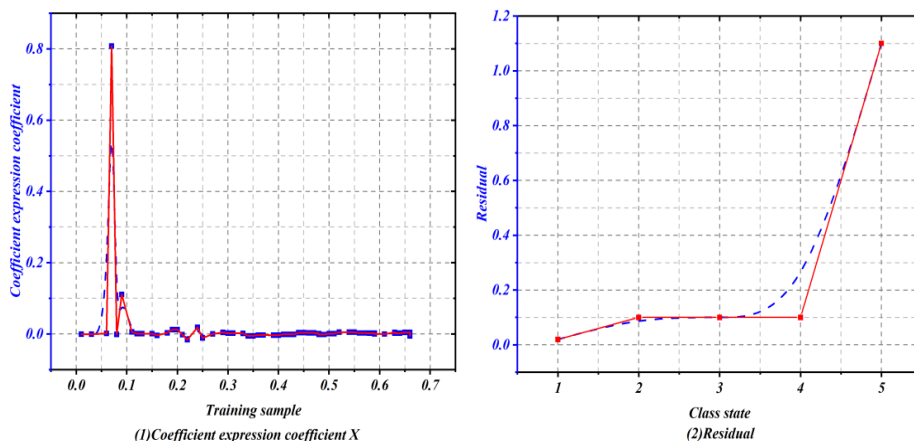


Fig. 2. Sparse Coefficient and Residual

The required solution $c(x)$ is based on the two probability values in Equations 3-5. The $p(c)$ can be obtained by calculating the frequency of each class marker c appears in the training sample set. However, it is difficult to calculate each value directly, and estimating all the values is an NP-hard problem.

The naïve Bayes classifier assumes that the property values of a sample instance are [18] independently of one another, given the instance of an instance. Therefore, the product of the probabilities of each individual attribute value is the joint probability distribution. Its formula is:

$$p(a_1, a_2, \dots, a_n | c) = \prod_{i=1}^n p(a_i | c) \quad (37)$$

According to formula 3-5 and formula 3-6, the classification formula of naive Bayes classifier can be expressed as:

$$c(x) = \underset{cec}{\operatorname{argmax}} \prod_{i=1}^n p(a_i | c)p(c) \quad (38)$$

As a_i is the i th attribute value of x , $p(a_i | c)$ and $p(c)$ can be estimated by calculating the occurrence frequency of different class markers and attribute value combinations in the training sample instance, as follows:

$$p(c) = \frac{\sum_{j=1}^n \delta(c_j, c)}{\sum_{j=1}^n \delta(a_{ji}, a_i) \delta(c_j, c)} \quad (39)$$

$$P(a_i | c) = \frac{\sum_{j=1}^n \delta(a_{ji}, a_i) \delta(c_j, c)}{\sum_{j=1}^n \delta(c_j, c)} \quad (40)$$

Where n represents the number of training sample instances; c_j represents the class marker of the j -th training sample instance; a_{ji} represents the i -th attribute value of the j -th training sample instance $\delta(c_j, c)$ represents the binary function, Its value is 1 when used in $c_j = c$.

In practice, Laplace estimates are often used to smooth Equations 39, and the probabilities obtained in Equations 40.

$$p(c) = \frac{\sum_{j=1}^n \delta(c_j, c) + 1}{n + q} \quad (41)$$

$$P(a_i | c) = \frac{\sum_{j=1}^n \delta(a_{ji}, a_i) \delta(c_j, c) + 1}{\sum_{j=1}^n \delta(c_j, c) + n_i} \quad (42)$$

And q is the number of class markers; n_i is the number of values of the i th attribute in the training sample instance. The above is the theoretical solution process of the naive Bayes classifier.

(2) Algorithm training

In this paper, 25 sets of data were collected by the data acquisition system for parameter learning. The common electrical system faults in actual buildings mainly include four categories: Circuit Impedance Failure, Earthing Failure, Isolation Failure, Continuous Failure, and Normal Condition of Architecture Electric System [19]. In this paper, 115 sets of sample data were collected through the experimental platform FSP. Each group sample is 10-dimensional data with 10 characteristic components of fault information at different locations. Among these, 50 groups were selected as training sample data, conditional probability distribution was calculated by naive Bayes classifier, 50 samples were used for parameter learning, and the remaining 15 groups were used as test samples.

As shown in Figure 3, when the line impedance fault occurs, namely the E1 state, the Bayesian network diagnosis model can diagnose the E1 fault before and after parameter learning. Before parameter learning, the probability of failure of E1, E2 and E3 is 0.835, 0.2443 and 0.3166 respectively. After parameter learning of the model, the probability of diagnostic failure in E1, E2, and E3 is 0.9147, 0.1648, and 0.2185 respectively. Its diagnostic accuracy has been significantly improved. The probability of failure in E4 and E5 is: 0.0917. And no change before and after parameter learning.

3.2. Classification of electrical equipment based on laser imaging technology

(1) Laser imaging technology

Laser detection of electrical equipment failure is a direct detection technique that can overcome atmospheric scattering with a high signal to noise ratio of active imaging systems. This technique separates the target reflected light from the backscattered light in time, so as to eliminate the influence of the backscattered light; when observing the target, improve the peak laser power and the sensitivity of the detection system to a certain extent, thus obtaining high target resolution and laser image quality [20].

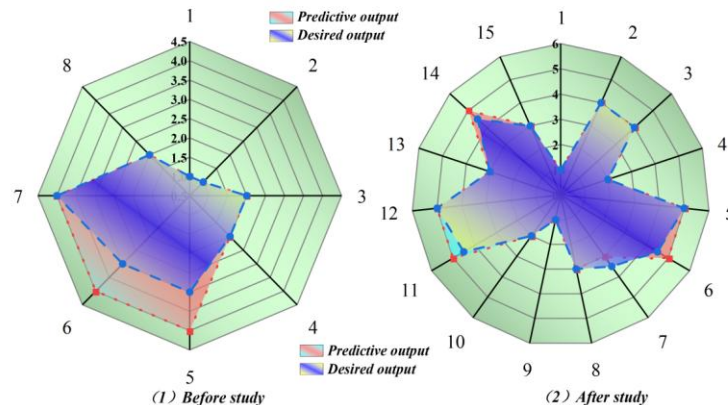


Fig. 3. Classification effects of Bayesian network models before and after parameter learning

Electrical equipment area to be detected is illuminated between the laser imager, in which a portion of the directed background laser is reflected camera, as shown in Figure 4 (1); If the electrical equipment fails, then the returned laser intensity is weakened due to the abnormal fault position, then the image in the fault area of the electrical equipment will form a more obvious contrast change. The more serious the fault, the weaker the returned laser intensity, and the more obvious the contrast. In this case, ordinary equipment faults can be seen in the monitoring video, and their positions can be determined. The imaging principle is shown in Figure 4 (2).

The theoretical mathematical expression for the maximum image resolution is:

$$\Delta R_m = \frac{c(\tau_p + \tau_s)}{2} \quad (43)$$

Where ΔR_m represents the maximum distance resolution; c represents the speed of light; τ_p represents the laser pulse width; τ_p and τ_s represents the detector gate width. The expression with the smallest image resolution is:

$$\Delta R_{me} = \begin{cases} \frac{c \cdot \tau_p}{2}, \tau_p > \tau_s \\ \frac{c \cdot \tau_s}{2}, \tau_s > \tau_p \end{cases} \quad (44)$$

Where: ΔR_{me} represents the minimum resolution.

If the laser pulse width is very narrow, the laser receiver can only receive the return laser around the target to be detected, which can greatly improve the signal-to-noise ratio of the return light wave, thus obtaining a higher resolution target image.

(2) Laser image processing

First, the image is stretched to a certain proportion of contrast, and the calculation formula of the stretch change is as follows:

$$f(x, y) = h \times \frac{g(x, y) - b}{a - b} \quad (45)$$

Where $g(x, y)$ represents the original gray level of the laser image; f represents the gray level after contrast stretching; h represents the largest gray level presented by the laser image after stretching; a and b represent the original gray level maximum and the original gray level minimum, respectively. After stretching transformation processing, the gray value range of the image is increased to strengthen its contrast.

back to the laser imager [21]. In the case of no failure, the resulting image is consistent with the backscattered light image taken by the ordinary

Let S_{xy} represent the coordinate group of rectangular subimage windows with center at (x, y) and size $m \times n$. The laser image denoising processing, choose the median filter, is a common nonlinear denoising processing method, mainly for salt and pepper noise, in some cases, it can remove the noise interference and make the image edge information is not damaged.

Median filtering - the core idea is to replace the median value of each point in the laser image with the median value of each point value in the area near the value, whose expression is:

$$f(x, y) = med_{(s,t) \in S_{xy}} \{g(s, t)\} \quad (46)$$

4. THE WINDOW OF 2 D MEDIAN FILTERING CAN BE RECTANGLE, CIRCLE AND CRUCIFORM. 4 ELECTRICAL FAULT CLASSIFICATION SYSTEM DRIVEN BY ARTIFICIAL INTELLIGENCE

4.1. Diagnostic system

Fig. 5 illustrates a general frame for constructing an electric failure diagnostic algorithm using WT-SVM.

Step 1: Eurotest61557 Collect the fault signal on the building electrical test platform;

Step 2: The collected original fault signal is denoised with Sym 4 wavelet, and the reconstructed signal is obtained and normalized;

Step 3: The processed signals are randomly selected to generate the training set and the test set. Training dataset occupies about 4/5 of the sample dataset, while the experimental dataset takes up one fifth of the sample;

Step 4: This chapter uses the Gaussian kernel function as the kernel function in the SVM algorithm, and uses the cross-validation method to determine the optimal kernel parameters;

Step 5: Set the threshold and diagnose the fault data with the SVM algorithm model;

Step 6: The training is over, and the results are obtained.

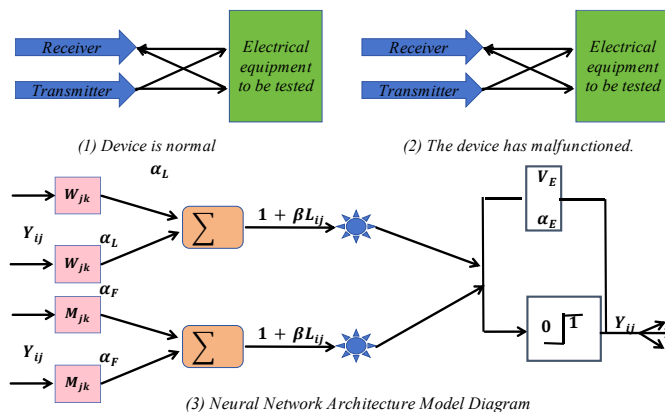


Fig. 4. Laser classification technique

4.2. Classification system

The electrical equipment fault diagnosis method studied in this paper is similar to that of cat mammals. It is a neural network of visual synchronous issuing pulses and compared to other networks of the same type. The neural network mentioned avoids complex training, and each neuron in the network corresponds to each pixel (i, j) in the laser image I, which will constitute a single-level processing system, and then realizes the extraction of the fault area according to the intrinsic mechanism of the neurons.

Figure 2 shows the model of the neuronal structure. The input of the neuron is divided into feedback input F and connected input L, which can receive the information of adjacent neurons and the laser image gray information.

Each partial input includes an electrical equipment fault integrator with similar exponential attenuation to ensure the relationship between the states of the neuron in various periods [14]. The expressions for the present state and the previous state are expressed as, respectively:

$$\bullet F_{ij}(n) = e^{-aF} F_{ij}(n-1) + I_{ij} + V_F \sum_{i/\in N_i} M_{i,u} Y_{ui}(n-1) \quad (47)$$

$$\bullet L_{ij}(n) = e^{-aL} L_{ij}(n-1) + V_L \sum_{i/k N_j} W_{ij,u} Y_{ud}(n-1) \quad (48)$$

$$\bullet M_{i,u}, W_{j,ul} = \begin{cases} 0, (i,j) = (k,l) \\ \frac{1}{\|(i,j)-(k,l)\|_2}, (i,j) \neq (k,l) \end{cases} \quad (49)$$

In: the goal of M and W is to transmit the pulse signal from adjacent neurons to the central neuron.

Then, in the case of nonlinear coupling, F and L will cause a series of changes in the intrinsic properties of the neurons. In general, the features within the neurons can be expressed as:

$$U_i(n) = F_i(n) \cdot [1 + \beta L_{ij}(n)] \quad (50)$$

$$Y_i(n) = \begin{cases} 1, U_i(n) > E_{ij}(n-1) \\ 0, other \end{cases} \quad (51)$$

In: E represents the dynamic threshold of the neurons itself, which also has the fault integrator characteristic with similar exponential decay [17], the expression is:

$$E_{ij}(n) = \exp(-\alpha_k) E_{ij}(n-1) + V_E Y_j(n-1) \quad (52)$$

Where: VE is constant. According to formula (10), it can be concluded that after the neuron ignition phenomenon occurs, the threshold value E will increase rapidly in a very short period of time and VE will change dynamically until the neuron appears ignition phenomenon again. So each neuron has a corresponding firing frequency. Due to the coupling connection between neurons, will be the nearby area similar neurons joint ignition phenomenon, thus form the neural network mentioned in this paper, at the same time on the laser image, the electrical equipment failure area brightness will be enhanced, using the mentioned neural network will light area reasonable extraction, which can ensure the original information of the laser image, and electrical fault area diagnosis.

The specific process of fault detection and classification of electrical equipment is as follows:

- (1) Sample the laser image of the electrical equipment, and obtain the original laser image information;
- (2) Use formula (7) stretching the contrast of the original laser image;
- (3) The median filter is used to denoise the laser image of the electrical equipment;
- (4) The neuronal network is used to extract the fault area of the equipment in the image;
- (5) Obtain the classification results of electrical equipment faults.

5. SYSTEM APPLICATION

5.1. Diagnose

This section uses a 64-bit Windows 10 operating system, processor Intel (R) Core (TM) i5-8500 CPU @ 3.00GHz, hardware environment with 8 GRAM, the software used in the experiment is MATLAB2018a. The experimental data in this chapter are all from the simulated fault data collected in the building electrical system platform MA2067. Among them, 4-10 fault test points were selected from 22 fault test points for relevant experiments.

First, Sym 4 wavelet function was used to transform the original fault signal and obtain the reconstructed signal. For convenient comparison, the simulation of the original signal and the residual signal in 400 and 800 respectively, as shown in Figures 5-6, the residual signal is the difference between the original signal and the reconstructed signal. The denoising process of other failure signals is the same principle.

From Figures 5-7, the volatility of the original data is large, and the value varies between 10.74658 and 10.75949 with a range of about 0.01291. After wavelet denoising, the volatility of the data decreases significantly, and the value varies between 10.74285 and 10.76477 with a range of about 0.02192. The goal of wavelet denoising is to eliminate high-frequency noise while retaining the main features of the signal. As can be seen from the data, the processed data is significantly deviated from the original data at some time points (such as time points 200 and 250), indicating that the wavelet denoising method may have successfully eliminated some of the noise. However, at some time points (e. g., time point 100), the processed data is actually higher than the original data, which may be because the wavelet denoising method introduces some errors in the processing process, or the frequency of noise overlaps with the signal frequency, resulting in unsatisfactory denoising effect.

Through simulation tests, 400,800,1200,1600 samples were selected, of which 80% were training and testing, and the training and test samples were randomly sampled to ensure the correctness of the trial results. Figures 8-11 is an identification simulation diagram of the proposed method for 4

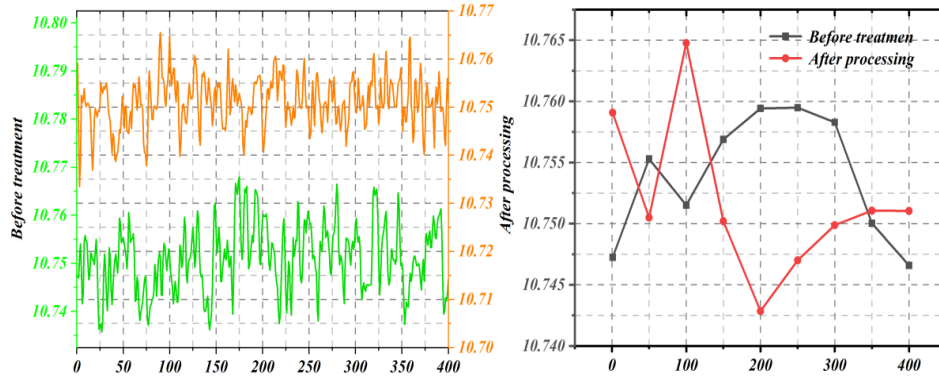


Fig. 5. Raw data

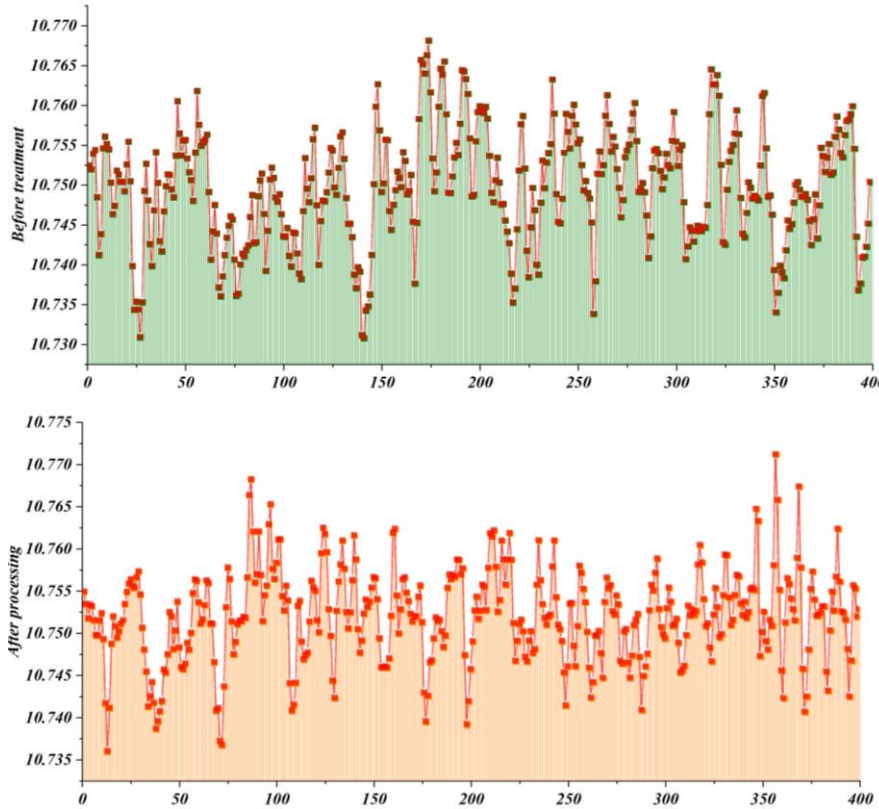


Fig. 6. Reconstructing the signal

types of failure types under various types of data sampling, where red represents the actual type and blue represents the predicted type. The systematic analysis of Figure 8 shows that when the small number of samples (0.33~10.98): the prediction results are close to the real results, and the error is small.

After the number of samples increased to more than 30, the error began to fluctuate, and even appeared obvious identification errors (e. g., 23.18, 29.13, 37.79, 46.21, etc.). It does not show that the accuracy of the prediction results increases significantly as the number of samples increases. By figure also can be seen: each sample identification accuracy are more than 70%, but when the number of samples increase, identification accuracy did not increase, the reason is that support vector machine in fault diagnosis, often need to find a surface to segment, and the number of data on the surface is not obvious, so no matter how big scale, the accuracy remains within a certain range.

Fig. 12 illustrates the four fault locations' training times for various sample data sizes. From the results of the simulation, we can find that the number of samples has little effect on the learning time, but Fig. 12 shows that the size of the sample has significant effect on the learning time. As the number of data increases, the training time is nearly doubled. For the purpose of further analysis of WT-SVM diagnosis, we will carry out a series of tests on the influence of the error type and the number of data. Fig. 12 (1) illustrates the relation between failure type and classification precision. To make sure that only one variable influences precision, we used a sample size of 400. From the experiment, it is found that under the same number of samples, the precision of the experiment group and the training group are higher than that under the condition that there are ten failures, the precision of the arithmetic, the precision of the training group is 81.4%, the test group is 80.3%, and in the 4 failures, the precision of the training group

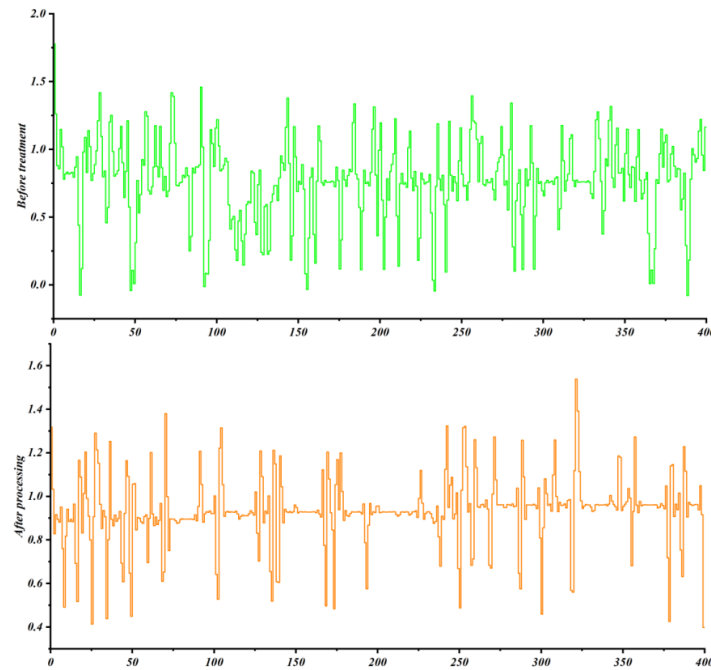


Fig. 7. Residues

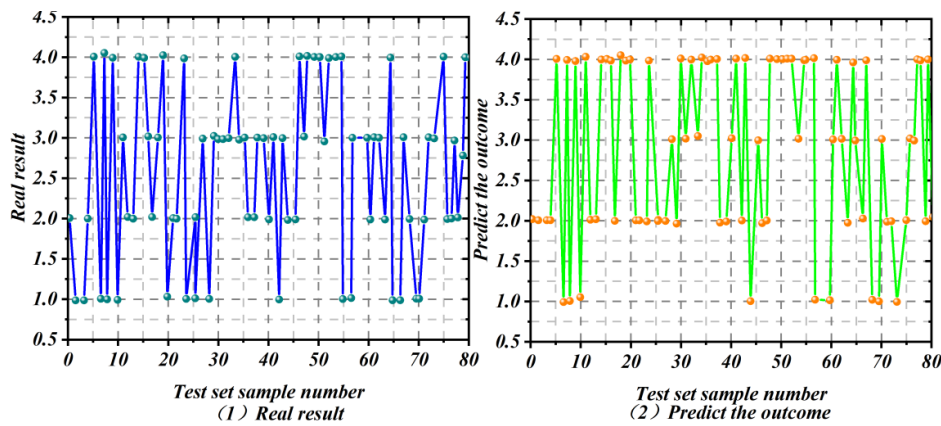


Fig. 8. classification result plot under 400 data samples

is 73.79%, and the precision of the test group is only 73.75%. So we can conclude that the WT-SVM electric system's failure diagnostic method is more efficient when there are many kinds of failures. From Figure 12 (2), when there are more kinds of failures, the performance of this method

To test the influence of the data set on SVM categorization, we have done an experimental study on the relation of the data set's size and precision in the case of ten failures. The results are illustrated in Graphs 3 - 18 and 3 - 19. From Figure 12 (3), when the sample is 400, the precision of the training dataset is 81.5% and the experimental dataset is 80.3%, and the precision of the training group is 82.1% and the experimental group is 81.5% at 2400. As a result, there is no significant difference between the precision of the experiment and the training group, which shows that the size of the sample has no effect on the precision of the method. As shown in Fig. 12 (4), however, as the number of sample data

increases, the time required for training also increases, and this is in line with the results obtained in the preceding four failure tests.

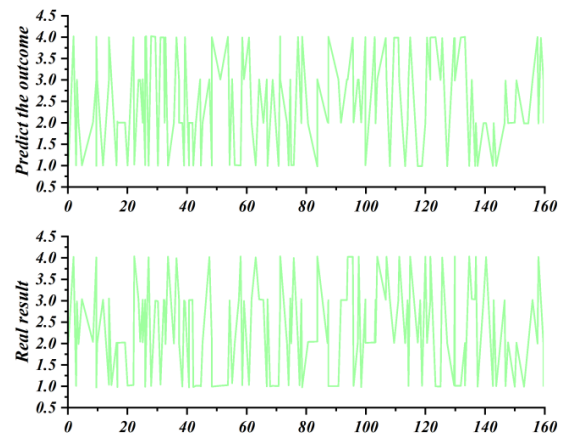


Fig. 9. 800 data samples is better than that of 400.

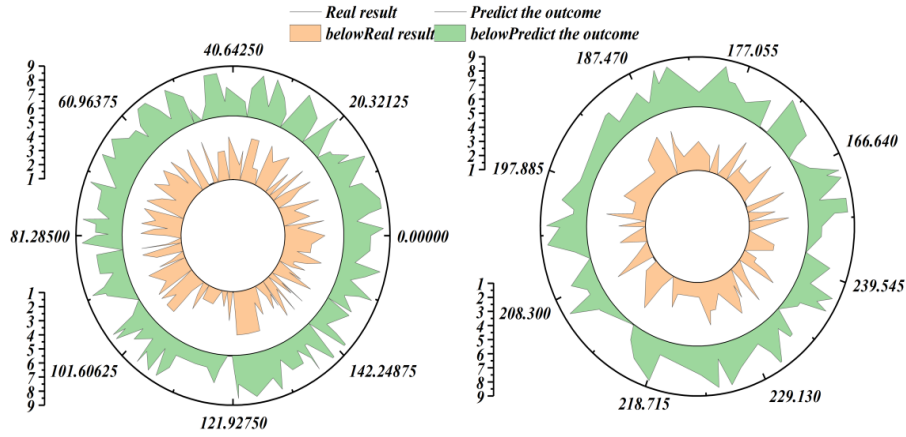


Fig. 10. Classification graph 1200 data samples

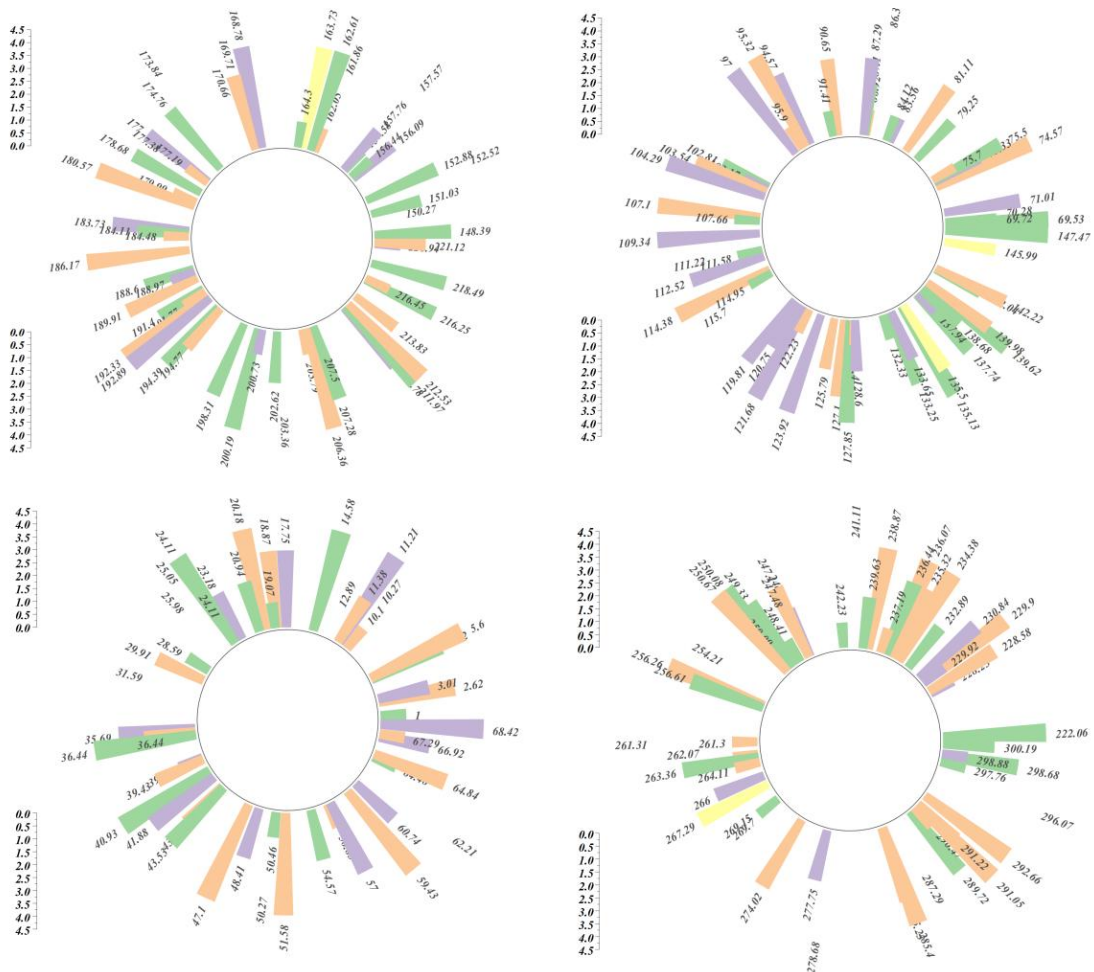
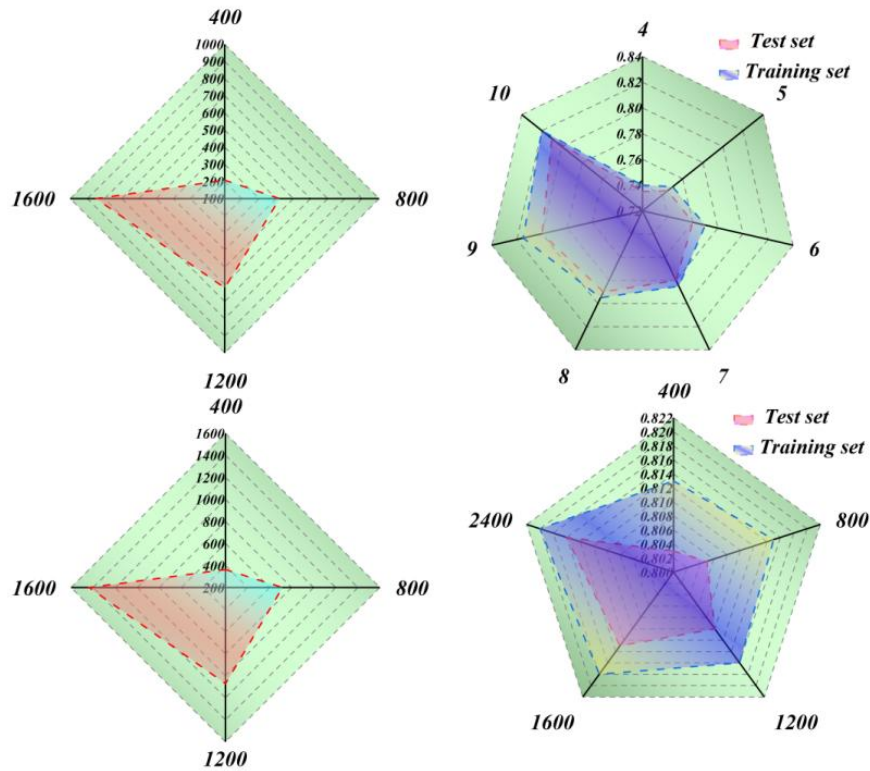


Fig. 11. 1600 data samples

5.2 Classify

To be able to demonstrate the feasibility of the studied automatic classification of electrical equipment failure methods, need to be configured as: processor Intel Xeon Gold6154 @ 3.00 GHz, Main board H110, The graphics card, GeForceGTX1050, Memory is 4 GB DDR4-2400, Solid-state 240 / 256 GBPCIe3. 0, Display: 7680x5120HDMI2. 1, the operating system creates a simulation experimental platform on the Windows 10's computer, Simulation experimental environment with the software as

Matlab 7. 1. For the sake of simplicity of the experiment, we adopt the first, second and third approaches instead of the simulated comparative test. The experiment object selected the electrical equipment in a factory in the city. The common faults of the equipment include excessive current, excessive voltage, overheating and grounding. Experimental sampling statistics of the electrical equipment monitoring system yielded 500 sets of sample data.



(1) Training time for different sample data sizes (2) Relationship between fault type and accuracy rate

Fig. 12. Training times for different sample data sizes

In the experiment, different electrical equipment faults in 4 were taken as the discussion objects of the methods, and the experimental subjects were classified by methods 1,2 and 3. The classification results are shown in Table 1. Where faults a, b, c and d indicate the excessive current, excessive voltage, overheating and ground faults in the electrical equipment respectively.

From Fig. 13, it can be found that there are two mistakes in Method 1, and Method 2 has an error count of 3, B, C, and D, and Method 2 has an error count of 0, which makes it possible to differentiate correctly between various types of failures.

To show that the proposed approach is stable in simulated test, we have carried out some tests on the

test subjects. The experimental index is the accuracy of the method, and the diagnostic results are shown in Figure 14:

Through the analysis of figure 14: the diagnostic accuracy is low, followed by method 2, and method 3 maintain high accuracy, and change trend into a smooth state, the highest accuracy value as high as 100%, the lowest value in around 90%, which can explain the study of electrical equipment fault automatic classification technology is relatively accurate, and high stability.

To further verify the automatic diagnostic fault classification, the following experiments were performed, and the experimental results are shown in Figure 15.

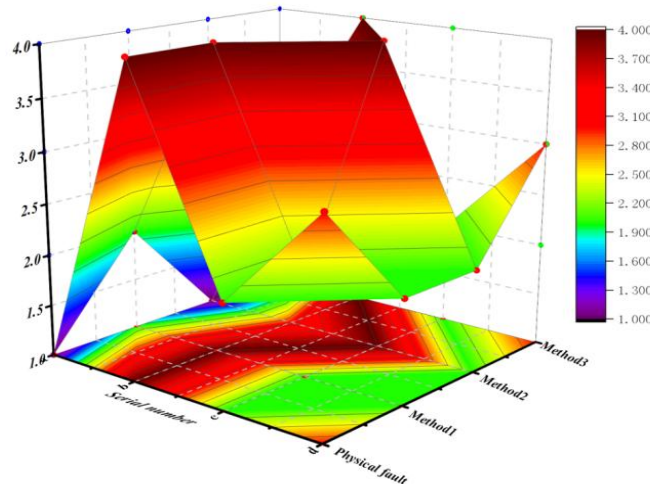


Fig. 13. Electrical equipment classification results for different methods

As shown in Figure 15, 60 sets of experimental data were randomly selected for automatic fault classification comparison. It can be seen from the comparison results that the method 3 classification time is the shortest, significantly lower than method 1 and method 2. Fully proved the advantage of the method.

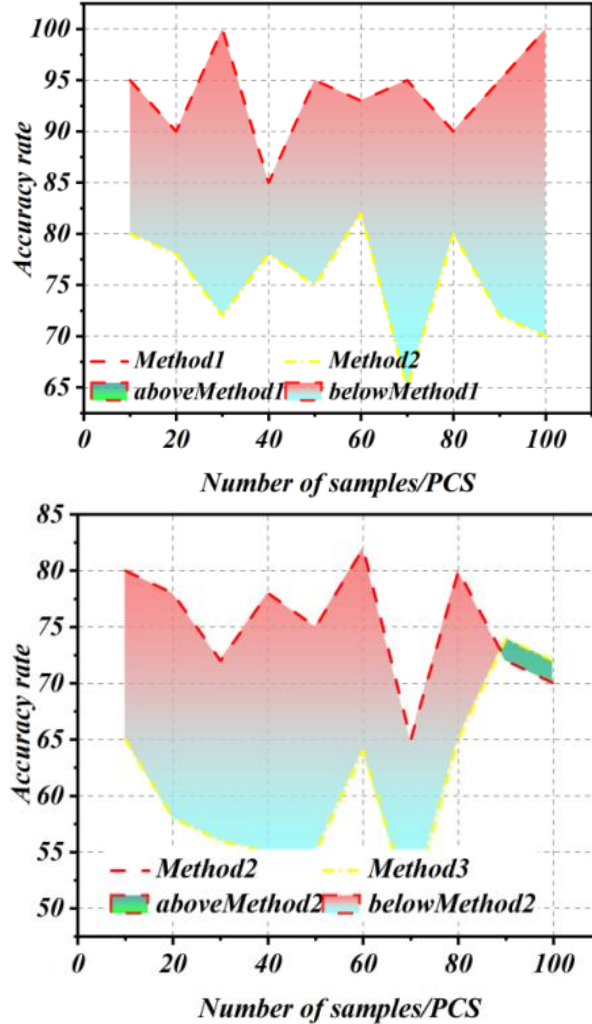


Fig. 14. Comparison of the diagnostic accuracy for the different methods

6 DISCUSSION

In this paper, we constructed an automatic electrical fault classification system based on Support Vector Machine (SVM) and Bayesian algorithm, and verified its effectiveness through experiments. However, compared with similar literature, the study still has some deficiencies, mainly reflected in the following aspects:

(a) Insufficient data diversity and sample size

This study is mainly based on small sample data. Although it performs well in small sample scenarios, in practice, the electrical failure types are complex and diverse, and the scale of the failure data is large. Similar literature points out that deep learning-based fault diagnosis methods can handle large-scale data and improve the classification accuracy through multi-source data fusion. However, this paper does

not involve the processing power of large-scale data, nor discusses the influence of data diversity on the classification effect. Future studies could consider introducing more types of failure data and explore data enhancement techniques to improve the generalization capability of the model.

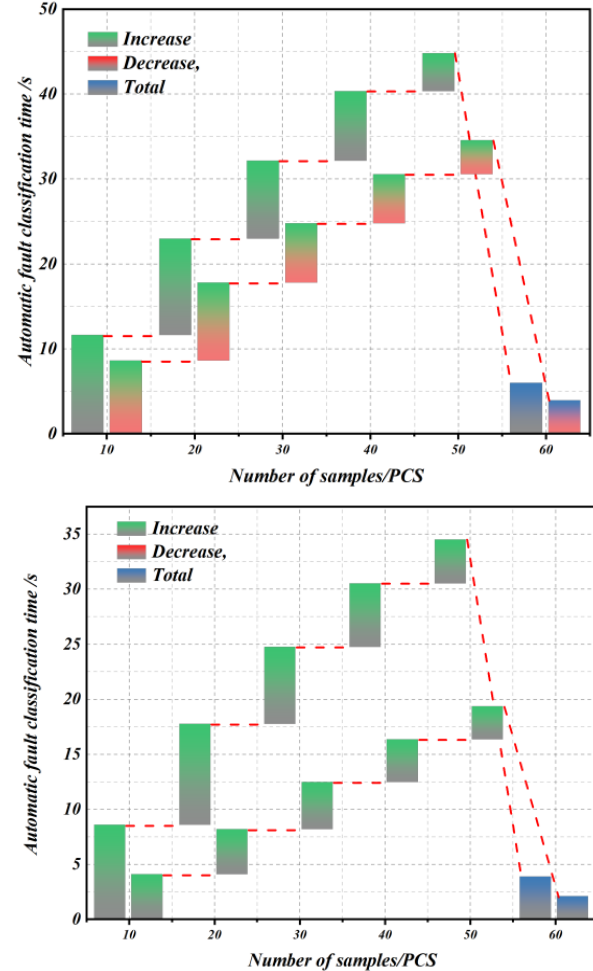


Fig. 15. Comparison of automatic fault classification of different methods

(b) Insufficient complexity and real-time performance of the algorithm

Although the proposed fault diagnosis algorithm based on wavelet transform and SVM has a high classification accuracy, especially when dealing with large-scale data, the training and inference time increase significantly. Similar fault diagnosis methods based on compressed sensing and deep learning mentioned in the literature perform better in real-time performance and computational efficiency. Therefore, future studies can try to introduce lightweight neural network or edge computing technology to improve the real-time performance and deployment efficiency of the system.

(c) Insufficient multimodal data fusion

This paper mainly relies on electrical signal data for fault diagnosis, and similar literature points out that the combination of multi-modal data (such as vibration signal, infrared image, temperature data,

etc.) can significantly improve the accuracy and comprehensiveness of fault diagnosis. For example, fault diagnosis methods based on laser imaging technology can effectively identify the physical defects of electrical equipment. Future studies can explore multimodal data fusion techniques to capture fault features more comprehensively.

(d) Insufficient explanatory power and reliability of the model

Although the algorithm proposed in this paper performs well in classification accuracy, its model is less explanatory, making it difficult to intuitively understand the decision process of fault classification. Similar methods based on expert systems and fuzzy theories mentioned in the literature have advantages in model interpretability and can provide an interpretable inference process for fault diagnosis. Future research could combine explanatory artificial intelligence (XAI) technology to improve the transparency and reliability of the model.

(e) Lack of system robustness and adaptability

The experimental environment in this paper is relatively ideal, without complicated factors such as noise interference and equipment aging in practical application. Similar literature states that deep-learning and reinforcement learning-based methods are more robust and adaptable in complex environments. Future studies could introduce robust optimization techniques and online learning mechanisms to improve the adaptability of the system in practical scenarios.

7 CONCLUSION

This study constructs an automated electrical fault classification system based on Bayesian algorithms, integrating wavelet transform, support vector machine, compressed sensing, and laser imaging technology. It systematically addresses the limitations of traditional methods in scenarios such as small sample data, noise interference, and insufficient real-time performance. In terms of methodology, wavelet transform is first used to perform multi-scale decomposition and denoising of electrical signals, effectively improving the signal-to-noise ratio. Next, a strategy combining support vector machine and relevance vector machine is adopted to optimize fault feature extraction and multi-class classification processes, while leveraging compressed sensing algorithms to enhance the processing capability for sparse signals. At the same time, Bayesian classifiers are introduced to quantify uncertainty factors, and laser imaging technology is combined with image enhancement and neural network localization analysis to form a diagnostic framework that integrates multimodal data. Experimental results show:

(1) The system performs well under the condition of small sample, and the average fault identification accuracy is more than 70%. Among them, the

feature extraction method based on wavelet transform shows the stability classification accuracy of 90%-100%. After parameter optimization, the Bayesian classifier further improves the fault diagnosis confidence to 91.47%, which verifies the robustness of the algorithm in the noisy environment.

- (2) The sample size has a limited impact on the classification accuracy, while the computational complexity increases exponentially with the data volume, indicating that the system has significant efficiency advantages in small sample scenarios.
- (3) By combining probability expression and sparse representation, the technology system can accurately identify five kinds of faults such as line impedance and ground resistance anomaly, which breaks through the bottleneck of traditional threshold method relying on empirical rules.
- (4) It provides a practical solution for fault prediction and health management of intelligent building power system. By reducing the false alarm rate and shortening the diagnosis time, it can effectively avoid equipment downtime and safety accidents, which has practical significance to promote the digital transformation of smart city power operation and maintenance. At the same time, it provides an interdisciplinary methodological reference for small sample fault diagnosis theory of complex systems.

Source of funding: *This paper was supported by Key Research Projects of Higher Education Institutions in Henan. Province Research and Application of Key Technology of Intelligent Protection Measurement and Control Terminal for Domestic Multicore Heterogeneous New Energy Box Transformer under grant No. 25B470016.*

Author contributions: *Research concept and design, X.Z.; Conceptualization and methodology M.Z.*

Declaration of competing interest: *The author declares no conflict of interest.*

REFERENCES

1. Wong JKW, Li H, Wang SW. Intelligent building research: a review. *Automation in Construction*. 2005; 14(1): 143-159. <https://doi.org/10.1016/j.autcon.2004.06.001>.
2. Zhao YF, Wang YH, Ren H, et al. Design of a data acquisition system for building electrical fault diagnosis. 27th Chinese Control and Decision Conference, Qingdao. 2015: 3355-3359. <https://doi.org/10.1109/CCDC.2015.7162500>.
3. Himmelblau DM. *Fault detection and diagnosis in chemical and petrochemical processes*. Amsterdam: Elsevier Science Limited. 1978:414.
4. Xiong JB, Zhang QH, Sun GX, et al. An information fusion fault diagnosis method based on dimensionless indicators with static discounting factor and KNN. *IEEE Sensors Journal*. 2015;16(7):2060-2069. <https://doi.org/10.1109/JSEN.2015.2497545>.
5. Zhao YF. Research of fault diagnosis method for

- building electrical. Beijing: Beijing University of Civil Engineering and Architecture. 2017.
6. Wang JJ, Wang YH. The research of building electrical fault diagnosis based on experimental platform. 2020 Chinese Control and Decision Conference, Hefei. 2020:2595-2599.
<https://doi.org/10.1109/CCDC49329.2020.9164018>.
 7. Wu Q, Wang Y H, Zhang L, et al. The research on fault diagnosis of building electrical system based on RBF neural network. 2013 Chinese Intelligent Automation Conference. Berlin: Springer. 2013:9-19.
https://doi.org/10.1007/978-3-642-38524-7_2.
 8. Zhang L, Chen C, Han N, et al. Fault diagnosis of electrical systems in buildings based on compressed sensing. CAAI Transactions on Intelligent Systems. 2014;9(2):204-209.
 9. Zhang L. The research on fault diagnosis of building electrical system. Beijing: Beijing Forestry University. 2014.
 10. Ding MJ. Design of electrical data acquisition system and study on fault diagnosis in residential building. Beijing: Beijing University of Civil Engineering and Architecture. 2015.
 11. Suthaharan S, Suthaharan S. Support vector machine. Machine learning models and algorithms for big data classification: thinking with examples for effective learning. 2016:207-235.
https://doi.org/10.1007/978-1-4899-7641-3_9.
 12. Ohenhen PE, Nwaobia NK, Nwasike CN, Gidiagba JO, Ani EC. Diagnostics and monitoring in electro-mechanical assemblies: assessing the latest tools and techniques for system health prediction. Acta Electronica Malaysia. 2024;8(1):11-20.
 13. Roy A, Chakraborty S. Support vector machine in structural reliability analysis: A review. Reliability Engineering & System Safety. 2023;233:109126.
<https://doi.org/10.1016/j.res.2023.109126>.
 14. Bansal M, Goyal A, Choudhary A. A comparative analysis of K-nearest neighbor, genetic, support vector machine, decision tree, and long short term memory algorithms in machine learning. Decision Analytics Journal. 2022;3:100071.
<https://doi.org/10.1016/j.dajour.2022.100071>.
 15. Tanveer M, Rajani T, Rastogi R, Shao YH, Ganaic MA. Comprehensive review on twin support vector machines. Annals of Operations Research. 2024; 339(3):1223-1268.
<https://doi.org/10.1007/s10479-022-04575-w>.
 16. Kurani A, Doshi P, Vakharia A, Shah M. A comprehensive comparative study of artificial neural network (ANN) and support vector machines (SVM) on stock forecasting. Annals of Data Science. 2023; 10(1):183-208.
<https://doi.org/10.1007/s40745-021-00344-x>.
 17. Almaiah MA, Almomani O, Alsaaidah A, Al-Otaibi S, Bani-Hani N, Hwaitat AKA, Aldhyani TH. Performance investigation of principal component analysis for intrusion detection system using different support vector machine kernels. Electronics. 2022; 11(21):3571.
<https://doi.org/10.3390/electronics11213571>.
 18. Avcı C, Budak M, Yağmur N, Balçık F. Comparison between random forest and support vector machine algorithms for LULC classification. International Journal of Engineering and Geosciences. 2023;8(1): 1-10. <https://doi.org/10.26833/ijeg.987605>.
 19. Zhang H, Zou Q, Ju Y, Song C, Chen D. Distance-based support vector machine to predict DNA N6-methyladenine modification. Current Bioinformatics. 2022;17(5):473-482.
<https://doi.org/10.2174/1574893617666220404145517>.
 20. Rodríguez-Pérez R, Bajorath J. Evolution of support vector machine and regression modeling in chemoinformatics and drug discovery. Journal of Computer-Aided Molecular Design. 2022;36(5): 355-362. <https://doi.org/10.1007/s10822-022-00442-9>.
 21. Zhang J, Zhang Q, Qin X, Sun Y. A two-stage fault diagnosis methodology for rotating machinery combining optimized support vector data description and optimized support vector machine. Measurement. 2022;200:111651.
<https://doi.org/10.1016/j.measurement.2022.111651>.



Xiaowei ZHANG, a member of the Communist Party of China, a university teacher, associate professor, director of the electrical team of the School of Mechanical and Electrical Engineering, a member of the National Mechanical Vocational Education and Teaching Steering Committee for Automation Technology, and a provincial backbone teacher of vocational colleges in Henan Province.

Main Works:

- Participated in the 2021 Henan Higher Vocational Education Skills Competition-Electromechanical Integration Project, won the first prize; led students to participate in the National Vocational College Skills Competition, won two national second prizes, two provincial first prizes; led students to participate in the National Vocational College Innovation and Entrepreneurship Competition, won two third prizes.

Membership in Academic Societies:

- Electrical team of the School of Mechatronics and Automotive Engineering.
- National Steering Committee for Mechanical Vocational Education and Training Steering Committee for Automation Technology.

e-mail: 13193461627@163.com



Mingdong ZHU, a member of the Communist Party of China, a university teacher, graduated from Hunan University with a major in Electrical Engineering, previously worked at Xuji Group Co., Ltd, having the Electrical Engineer Certificate issued by the People's Government of Xuchang City, and the

electrician vocational skill level certificate issued by Xuchang Vocational Technical College.

Main Works:

- Participated in the Electrical Engineering Competition of the 2024 Xuchang Vocational Skills Competition and won the Excellence Award; Led the students to participate in the final of the 2024 the Belt and Road and BRICS Power System Automation and New Energy Technology Competition, and won the third prize.

Membership in Academic Societies:

- The Electrical Automation Team of the college of Mechatronics and Automotive Engineering.

e-mail: MingdongZhu1542@outlook.com